

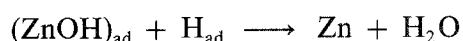
# Effect of PbO on zinc electrodeposition from zincate solutions

Z. MAO, S. SRINIVASAN, A. J. APPLEBY

*Center for Electrochemical Systems and Hydrogen Research, Texas Engineering Experiment Station, Texas A&M University System, College Station, TX 77843-3577, U.S.A.*

Received 1 April 1991; revised 25 November 1991

The effect of PbO on zinc electrodeposition on a copper substrate from zincate solutions was investigated using cyclic voltammetry and by polarization measurements as a function of time. It was found that lead deposition caused the zinc deposition potential to cathodically shift by 100 mV in the negative direction. It is suggested that the presence of lead on the copper substrate suppresses hydrogen absorption and consequently inhibits zinc deposition via a path such as



The polarization studies indicate that co-deposition of lead does not affect zinc deposition kinetics.

## 1. Introduction

Lead oxide (PbO) is one of the most common inorganic additives used in alkaline secondary batteries with zinc anodes [1, 2]. The beneficial effects of PbO on the zinc electrode include extension of cycle life, suppression of self-discharge rate, and an increase in cell capacity [3]. Therefore, the effects of PbO on zinc deposition and dissolution have become the subject of several studies [4-11]. The substrate effect and codeposition have often been cited as the causes for the beneficial effects of PbO. Lead deposited on the electrode becomes the substrate; the high hydrogen evolution overpotential on lead reduces self discharge rate. When lead codeposits with zinc during charge, the overpotential for zinc deposition is increased, which results in a denser deposit, and a more uniform current distribution with suppression of zinc dendrite formation.

Three types of experiment were conducted in previous investigations. In the first, PbO powder was directly added to ZnO paste [5, 8, 10]. Since PbO is slightly soluble in concentrated alkaline solution and some PbO also becomes detached from the electrode after a number of cycles [10], it is difficult to elucidate how the added PbO affects zinc deposition and dissolution during charge and discharge using this method. In the second, pure lead was used as the working electrode [6, 7]. In this case, the substrate effect of the metal can be observed. In the third, PbO was added to the electrolyte [4, 9]. In these experiments, the effect of PbO on zinc electrodeposition was examined on different substrates by cyclic voltammetry and by steady state polarization. It was generally found that the overpotential of zinc deposition increased due to the presence of PbO in the electrolyte. However, it appears that in this work certain precautions were not taken to prevent the situation in which electrodeposition of zinc occurs on the electrodes fully covered by deposited

lead, the deposition potential of which is more positive than that of zinc. Consequently, the conclusions for the third type of experiments were similar to those from the second type.

In the present work, cyclic voltammetry and polarization measurements as a function of time were employed to investigate the effect of PbO in zincate solutions on zinc electrodeposition on a copper substrate. Cyclic potential sweeps were carried out at different scanning rates within various potential envelopes, so that the electrode surface could be controlled at different desired states. Three types of electrode surface may be created by controlling the potential region and scanning rate, namely, those having little or no lead present, those partially covered by lead but periodically renewed and those on which lead coverage continuously increases. The electrochemical behaviour of zinc deposition on these surfaces may provide useful information about the effect of PbO on zinc electrodeposition. If lead codeposition with zinc directly affects zinc deposition, the current density due to the latter would be expected to decrease faster with time at a constant potential compared to that in the absence of PbO if the reaction is kinetically controlled. Therefore polarization measurements were made at different times, and compared with those in the absence of PbO to determine the effect of lead codeposition.

## 2. Experimental details

The electrolytes were prepared using deionized water with analytical grade potassium hydroxide pellets, ZnO and PbO powder. All the experiments were conducted in 12 M KOH solutions containing a range of ZnO and PbO concentrations. A pure copper wire, 1.05 mm in diameter and insulated in a thermal shrinkable Teflon tube, was used as the working electrode. Only the cross-sectional area of the wire was exposed

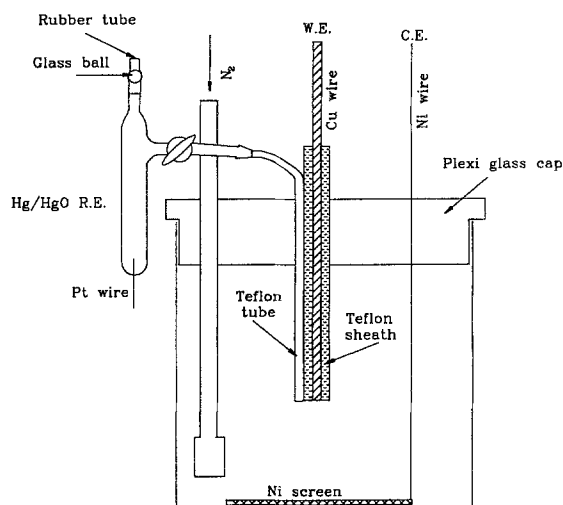


Fig. 1. Schematic view of the experimental cell.

to the electrolyte. The electrode surface was first polished with various grades of emery papers and finally polished on a polishing pad with  $1\ \mu\text{m}$  and  $0.05\ \mu\text{m}$  alumina. Copper was chosen because foam substrates of this metal have yielded promising results with flow-through rechargeable zinc electrodes [12, 13].

A one-compartment Pyrex glass cell was used in the experiments (see Fig. 1). The working electrode was mounted on the cap with the surface vertically facing the bottom. To maintain the same distance between the working electrode and the reference electrode for all experiments, the reference electrode was connected to one end of a 1 mm diameter flexible Teflon tube which was held parallel to the wall of the working electrode by Teflon tape. The reference electrode was Hg/HgO in 12 M KOH solution. The counter electrode was a nickel gauze placed on the bottom of the cell. During the experiments, nitrogen gas was continuously bubbled through the electrolyte. All the experiments were carried out at room temperature (about  $22^\circ\text{C}$ ).

The electrochemical instruments used in the experiments included a PAR Model 173 potentiostat/galvanostat, a PAR Model 175 programmer, and a Model 680 coulometer (Electrosynthesis Co.). The current responses to sweeping potentials in cyclic voltammetric experiments and to potential steps in polarization measurements were recorded with a X-Y recorder and a chart recorder, respectively.

### 3. Results and discussion

Figure 2 shows the cyclic voltammograms within a large potential range with and without PbO in the electrolyte. The anodic peaks at  $-0.1\ \text{V}$  in Fig. 2(a) may be due to the oxidation of the copper substrate, whereas the cathodic peak at  $-0.75\ \text{V}$  may correspond to the reduction of the resulting ionic copper species. The small anodic peak at  $-0.35\ \text{V}$  may be due to dissolution of surface alloyed zinc (i.e. a brass alloy) since a small amount of this may be formed during the previous cathodic sweep. This peak as well as the one at  $-0.75\ \text{V}$  only appears when the potential is scanned

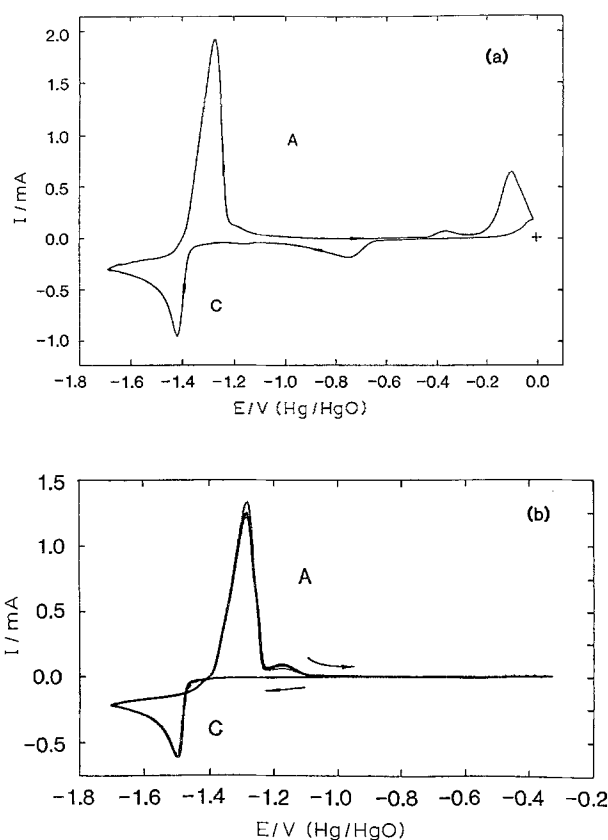


Fig. 2. Voltammograms at  $v = 20\ \text{mV s}^{-1}$ , (a) solution: 12 M KOH + 1 M ZnO; (b) solution: 12 M KOH + 1 M ZnO +  $3.58 \times 10^{-4}\ \text{M PbO}$ , electrode area  $8.66 \times 10^{-3}\ \text{cm}^2$ .

into a region more positive to  $-0.2\ \text{V}$ , where the copper dissolution can occur. However, any alloy formation can be superficial (1 or 2 monolayers at most) due to the slowness of solid state diffusion compared with the electrolytic reaction rates). The cathodic and anodic peaks near  $-1.4\ \text{V}$  are those for zinc deposition during the negative potential sweep and zinc dissolution in the following positive sweep. When the electrolyte contains PbO, the cathodic peak for zinc deposition is shifted by about  $100\ \text{mV}$  in the negative direction. These two voltammograms show the general effect of PbO in the electrolyte, and are consistent with the results reported by Melnicki *et al.* [4] and by McBreen *et al.* [6]. However, more detailed studies were needed to determine whether the effects observed are due to lead deposition on the substrate prior to zinc, or due to lead co-deposition with zinc.

It was observed that the redox reaction of copper at  $-0.1\ \text{V}$  has a significant effect on zinc deposition. When a potential of  $0.0\ \text{V}$  was applied before a negative sweep, an appreciable cathodic current started to appear near  $-1.0\ \text{V}$  rather than at the normal value of  $-1.37\ \text{V}$ . Chu *et al.* [7] have suggested that zinc undergoes an underpotential deposition on copper. It appears in this case that activated copper is responsible for zinc underpotential deposition since the cathodic current at  $-1.0\ \text{V}$  was not observed unless the potential was first maintained at  $0.0\ \text{V}$ . Nevertheless, to isolate the effects of PbO, interference from the copper substrate must be minimized. In addition, zinc electrodes in a practical battery will not be operated at potentials

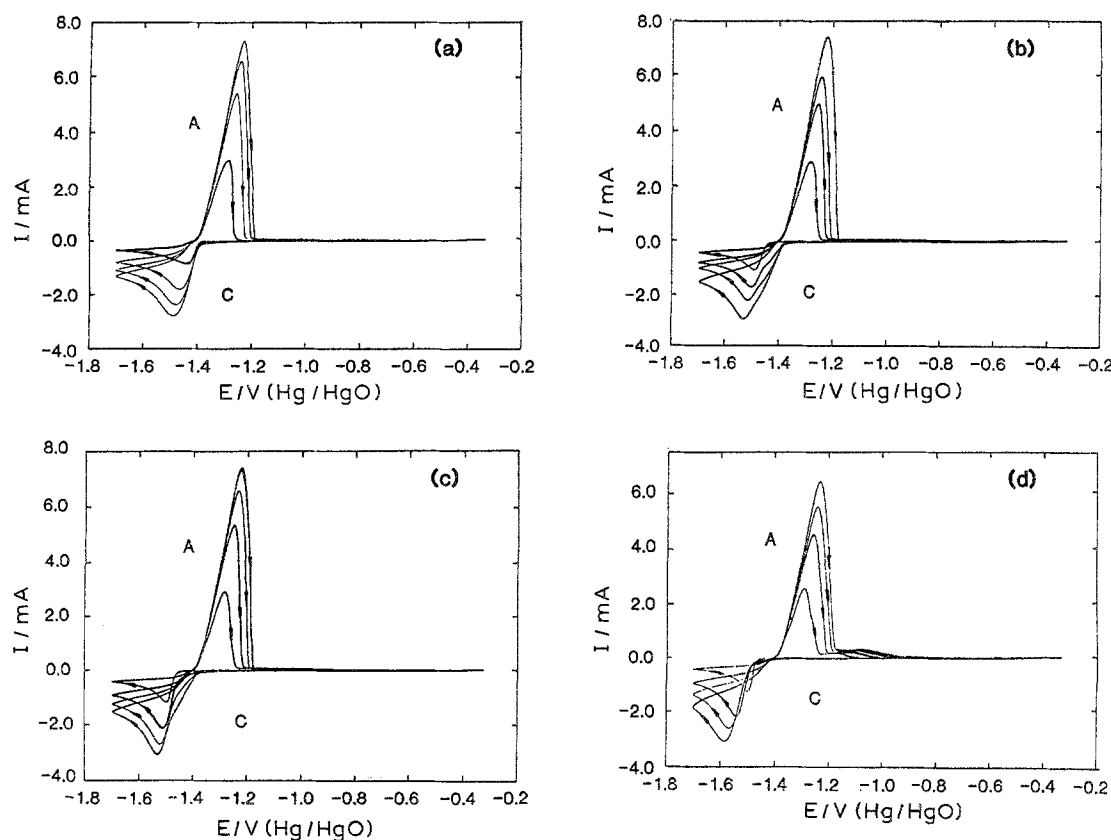


Fig. 3. Voltammograms at four scan rates: 20, 100, 200, 300  $\text{mVs}^{-1}$ . (a) 12 M KOH + 1 M ZnO; (b) 12 M KOH + 1 M ZnO +  $8.95 \times 10^{-3}$  M PbO; (c) 12 M KOH + 1 M ZnO +  $1.79 \times 10^{-4}$  M PbO; (d) 12 M KOH + 1 M ZnO +  $3.58 \times 10^{-4}$  M PbO. Electrode area  $8.66 \times 10^{-3}$   $\text{cm}^2$ .

where copper will be oxidized. Therefore, the electrode potential must be limited to a region where only zinc and lead deposition and dissolution occur.

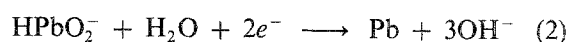
Figure 3 shows four groups of steady state voltammograms for different PbO contents at four scan rates. Without PbO in the electrolyte, the magnitude of the peaks increases with potential scan rate, but the shape of the voltammogram remains the same. With PbO in the electrolyte, the current on the leading edge of the cathodic peak decreases progressively with decreasing potential scan rate, and the threshold potential for zinc deposition is shifted cathodically by about 100 mV compared to the results obtained in the absence of PbO in the solution. Additionally, the current on the leading edge of the cathodic peak decreases with PbO content at a same scan rate. It should be noted that no appreciable current for lead deposition appears on the cyclic voltammograms, in spite of the large effects of PbO. A possible reason for this is that the current for lead deposition is too small to be measured at this degree of current sensitivity, since its limiting current may be estimated as being about two orders of magnitude smaller than those measured for zinc deposition: for example, if the diffusion coefficient of the lead ionic species is  $1.0 \times 10^{-5}$   $\text{cm}^2/\text{s}$ , the diffusion layer thickness is  $10^{-3}$  cm, and the limiting current for the lead deposition can be estimated using the equation:

$$I_{\text{lim}} = AnFD \frac{C}{\delta} \quad (1)$$

where the symbols  $A$ ,  $D$ , and  $C$  represent the electrode surface area, the diffusion coefficient and concentra-

tion of the reactant, respectively; the limiting current is about  $6.0 \times 10^{-3}$  mA, whereas the peak currents for zinc deposition are about 1 mA.

Since all of the solid PbO added to the electrolyte was completely dissolved, the resulting ionic species may be predominantly biphosphate ions ( $\text{HPbO}_2^-$ ) [14]. Lead deposition occurs according to the reaction



The equilibrium potential for the above reaction versus the Hg/HgO reference electrode can be expressed by the following equation, derived using the thermodynamic data at 25°C in [14]:

$$E = -0.637 + \frac{RT}{2F} \ln \frac{[\text{HPbO}_2^-]}{[\text{OH}^-]} \quad (3)$$

The lead deposition potential can be estimated to be approximately  $-0.78$  V at the PbO concentration in this experiment. Therefore, if the kinetics are rapid, lead would be continuously deposited on the copper substrate when the electrode potential became more negative than  $-0.8$  V during the potential sweep. Consequently, the results presented in Fig. 3 can be explained as the 'substrate effect'. At lower scan rates, more lead will be deposited, giving a greater effect on zinc deposition. Similarly, lead deposition will be proportional to the amount of PbO in the electrolyte.

Although the shapes of the cyclic voltammograms were strongly affected by the presence of PbO, its effect on the magnitude of both cathodic and anodic peaks is insignificant. Figure 4 shows that the cathodic peak heights are a linear function of the square root of

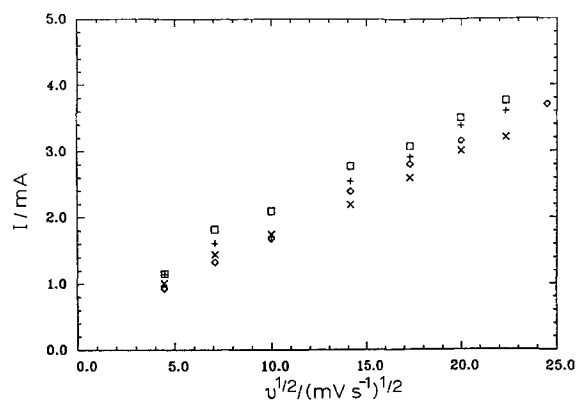
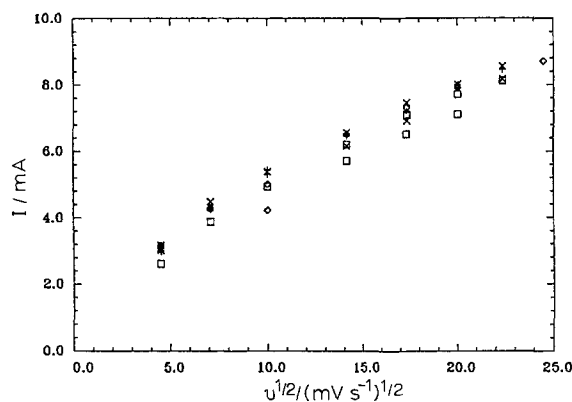
(a) Cathodic peak current vs.  $v^{1/2}$  at steady state(b) Anodic peak current vs.  $v^{1/2}$  at the first cycle

Fig. 4. The relationship between the peak current and square root of the scan rate. Electrode area  $8.66 \times 10^{-3} \text{ cm}^2$ . PbO content: ( $\square$ ) 4, (+) 2, ( $\times$ ) 1 and ( $\diamond$ ) 0 mg in 50 ml of 12 M KOH + 1 M ZnO solution.

potential scan rate, which indicates that the mass transport of zinc species limits the peak current. There is some dependence of the peak current on PbO content, but it is not consistent. The deviations may therefore be attributed to experimental error. For the anodic currents, it appears that depletion of the deposited zinc, rather than mass transport or surface passivation, limits the peak magnitude even though the linear relationship between the anodic peak current and the square root of the scan rate still holds. Figure 5 shows the ratio of the charge passed under the cathodic peak to that under the anodic peak. It is almost unity, indicating that the zinc deposited during

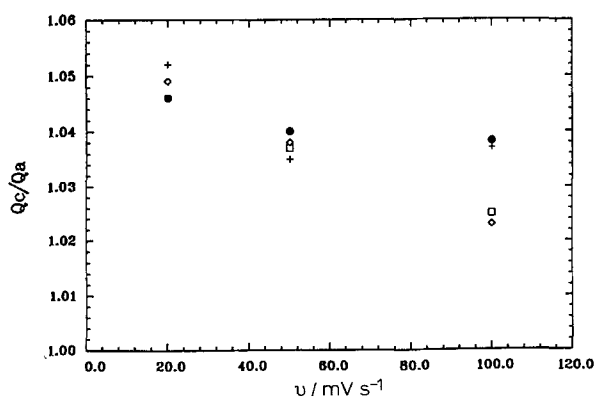


Fig. 5. The ratio of the total charge under the cathodic peak to that under the anodic peak versus the potential scan rate. PbO content: ( $\bullet$ ) 0, ( $\square$ ) 1, (+) 2 and ( $\diamond$ ) 4 mg in 50 ml of 12 M KOH + 1 M ZnO solution.

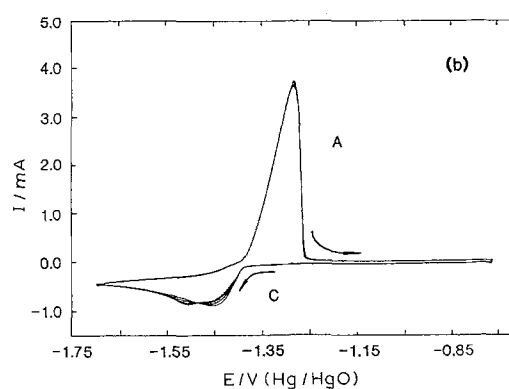
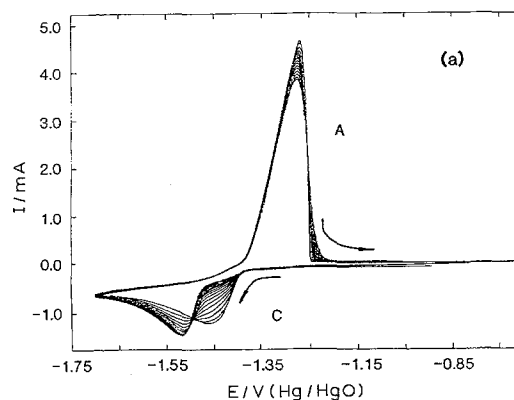


Fig. 6. Voltammograms with two potential regions, (a)  $v = \sim -(0.8-1.7) \text{ V}$ ; (b)  $v = \sim -(0.3-1.7) \text{ V}$ , Electrolyte: 12 M KOH + 0.5 M ZnO +  $1.79 \times 10^{-4} \text{ M PbO}$ , electrode area  $8.66 \times 10^{-3} \text{ cm}^2$ .

the negative potential sweep is completely dissolved in the electrolyte during the next positive sweep.

Figure 6 shows a comparison of two cyclic voltammograms with different potential limits. In Fig. 6(a), the electrode potential was scanned continuously within the envelope between  $-0.8 \text{ V}$  to  $-1.7 \text{ V}$ . As was already shown, lead will be continuously deposited in this potential region. As a result, the cathodic peak at  $-1.4 \text{ V}$  was gradually suppressed, and simultaneously the peak at  $-1.5 \text{ V}$  was enhanced, so that the cathodic peak was eventually shifted from  $-1.4$  to  $-1.5 \text{ V}$ . There appear to be two zinc deposition reactions, one occurring on the copper substrate and the other on lead, though at a more negative potential. However, it should be noted that these two peaks are strongly correlated, since the current at  $-1.5 \text{ V}$  did not increase without a simultaneous decrease in that at  $-1.4 \text{ V}$ . Evidently, when the rate of the reaction occurring at  $-1.4 \text{ V}$  is reduced, the reactant is readily converted into that for the reaction at  $-1.5 \text{ V}$ . As a result, the sum of concentrations of the two reactants for zinc deposition appears to be the same. In Fig. 6(b), the potential scan region was from  $-0.3$  to  $-1.7 \text{ V}$ , change in the voltammogram shape is not as significant as that in Fig. 6(a), and a steady state is reached after a few cycles. This may be attributed to the fact that the deposited lead is anodically dissolved and the electrode surface is periodically renewed.

When the relative concentration of PbO to ZnO in the electrolyte is increased, both zinc deposition and dissolution are significantly affected by the lead deposit,

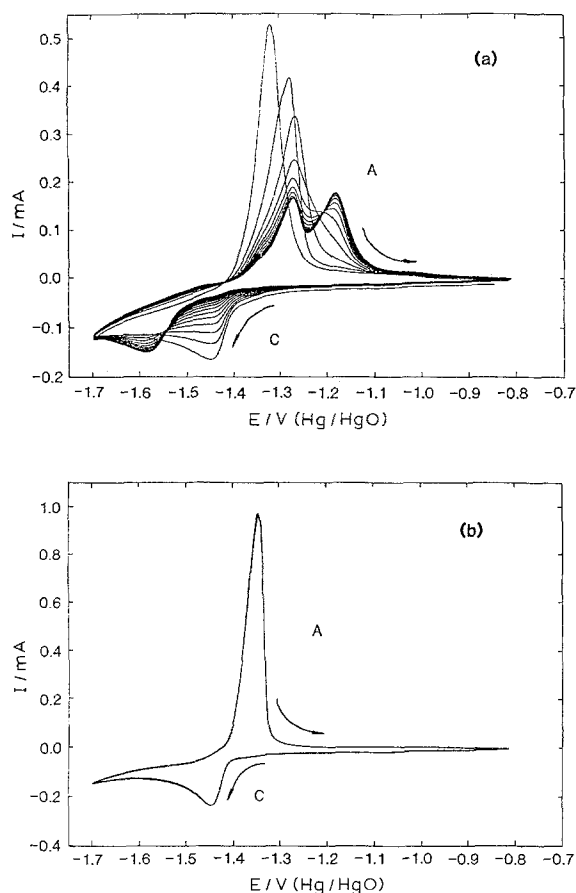
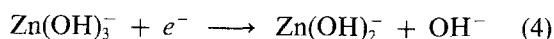


Fig. 7. Voltammograms at a scan rate of  $100 \text{ mV s}^{-1}$ . (a) solution:  $12 \text{ M KOH} + 0.1 \text{ M ZnO} + 1.79 \times 10^{-4} \text{ M PbO}$ ; and (b) solution:  $12 \text{ M KOH} + 0.1 \text{ M ZnO}$ .

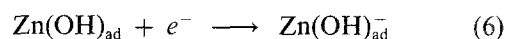
as Fig. 7(a) shows. To a greater extent than in Fig. 6(a), the cathodic peak near  $-1.4 \text{ V}$  was rapidly suppressed after a few cycles, whereas the second cathodic peak occurred at a more negative potential than that in Fig. 6(a). Additionally, the anodic peak was progressively shifted in the positive direction and finally split into two peaks. As lead accumulates on the surface during cycling, different zinc layers may be formed, which are responsible for the different dissolution peaks. Figure 7(b) shows a control voltammogram without PbO in the electrolyte. Only one cathodic and one anodic peak appears and each cycle exactly reproduces the previous one. The first cycle in (a) is almost identical to that in (b), and it is clear that the effect of lead on zinc deposition is proportional to the amount deposited on the surface.

The information about the effects of PbO shown by these cyclic voltammograms provides an opportunity to discuss the reaction mechanism of zinc deposition from zincate solutions, which has been extensively investigated [15–20]. Three mechanisms have been previously proposed. Bockris *et al.* [15] and Hendriks *et al.* [16] proposed a four-step mechanism for zinc deposition on zinc substrate, in which the rate-determining step is

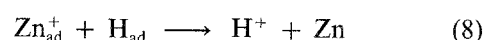
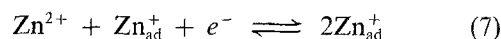


All the other mechanisms involve adsorbed species, such as reduced zinc and hydrogen. The mechanism proposed by Dirkse [17] and Farr and Hampson [18],

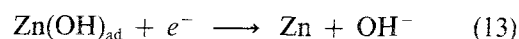
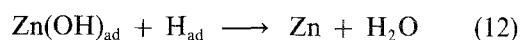
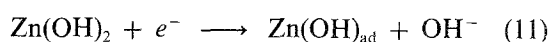
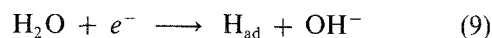
also consists of four steps and involves the reduction of adsorbed zinc species and the incorporation of zinc into kink sites as the rate determining steps. These reactions are



Based on S-shaped steady state polarization curves, Wiart and his co-workers [19, 20] proposed a multiple step model which involves the autocatalytic reaction and chemical reaction as follows:



This model was for acid solutions, but the impedance measurements and polarization plots for zinc electrodes in alkaline zincate solution are also similar to those in acidic solutions. Some combination of the models proposed by Hampson *et al.* and Wiart *et al.* may provide explanation for the cyclic voltammetric behavior observed in this work. Zinc deposition proceeds in a path, as follows:



Since the zinc deposition potential is much more negative than that for hydrogen evolution, Reaction 9 always occurs. When the electrode surface is free of lead, Reaction 12 may proceed, yielding a low overpotential for zinc deposition. When the electrode surface is progressively covered by deposited lead, Reaction 12 will be gradually suppressed, because hydrogen adsorption will become small [21]. Thus, zinc deposition would depend progressively on Reaction 13, which may occur at a more negative potential. Since Reactions 10 and 11 are considered to be fast, the limiting current would be due to the limited rate of zincate ion transport to the electrode surface, which would not be affected by the presence of lead on the electrode surface, as is shown in Fig. 4.

To determine whether the co-deposition of lead with zinc affect the electrodeposition of zinc, polarization curves were taken at different times from different groups of chronoamperometric curves. The results are shown in Fig. 8. Since the presence of lead on the electrode surface significantly affects the zinc deposition behavior as the voltammograms in the early figures show, it is important to use the same electrode surface for each potential step. The electrode potential was preset to a desired value for a certain period of time before a potential step was superimposed using values at  $-0.3 \text{ V}$  and  $-1.0 \text{ V}$ . At  $-0.3 \text{ V}$ , metallic lead is not stable, the electrode surface would be

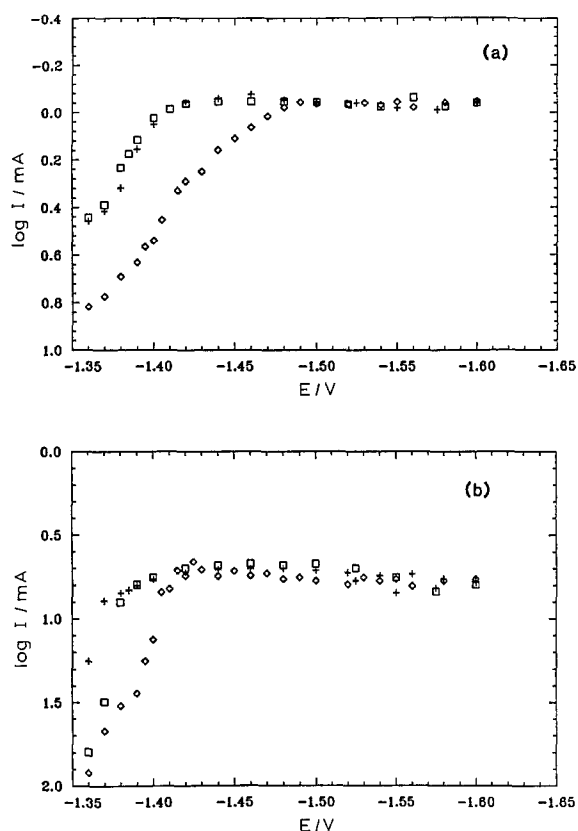


Fig. 8. Polarization curves. Solution: 12 M KOH + 0.5 M ZnO +  $1.79 \times 10^{-4}$  M PbO. (a) currents taken from the initial response to the potential steps; (b) current taken at 10 s after potential steps were applied. (□) Without PbO, (+)  $E$  rests at  $-0.3$  V and (◇)  $E$  rests  $-1.0$  V.

free of lead prior to the application of a potential step. At  $-1.0$  V, lead would be deposited on the electrode surface in amounts proportional to length of time during which the potential is preset. The chosen time was 5 s. Figure 8(a) shows that the currents are the same at any potential for the electrode surface free of lead whether or not the electrolyte contains PbO. However, the currents decreased significantly in a low potential region for the electrode surface carrying lead when the potential was preset at  $-1.0$  V. Figure 8(b) shows the polarization curves in which currents were taken at 10 s after a potential step was applied to the electrode. The differences shown in Fig. 8(a) for the three curves were apparently decreased as the zinc deposition time increased. It may be concluded that the co-deposition of lead with zinc does not significantly affect zinc deposition.

#### 4. Conclusions

The effect of PbO in zincate solutions on zinc electro-deposition has been shown to be via the 'substrate effect'. Lead is deposited on the substrate prior to zinc, so that the deposit serves as the substrate for zinc

deposition which causes the zinc deposition potential to cathodically shift by 100 mV. Lead codeposition does not significantly affect the zinc deposition potential. Chemical steps which involve reaction between adsorbed zinc species and adsorbed hydrogen atoms may be inhibited by the lead presence on the electrode surface.

#### Acknowledgement

This work was funded by Texas Higher Education Coordinating Board under Energy Research in Application Program, Contract No. 32121-70360 ERG.

#### References

- [1] F. R. McLarnon and E. J. Cairns, *J. Electrochem. Soc.* **138** (1991) 645.
- [2] J. McBreen and E. J. Cairns, 'Advances in Electrochemistry and Electrochemical Engineering', (edited by H. Gerischer and C. W. Tobias), John Wiley & Sons, New York (1978).
- [3] A. Himy and O. C. Wagner, *US Patent 4084047* (April, 1978).
- [4] L. S. Melnicki, I. Lazic, and D. Cipris, 'Role of Additives in Minimizing Zinc Electrode Shape Change: The Effect of Lead on the Kinetics of Zn(II) Reduction in Concentrated Alkaline Media', Final Report to Office of Naval Research, Contract N00014-82-0701 (1985), DTIC file No. AD-A158 806.
- [5] J. McBreen and E. Gannon, *Electrochimica Acta* **26** (1981) 1439.
- [6] J. McBreen, M. G. Chu and G. Adzic, *J. Electrochem. Soc.* **128** (1981) 2289.
- [7] M. G. Chu, J. McBreen and G. Adzic, *ibid.* **128** (1981) 2281.
- [8] R. L. Deutscher, S. Fletcher, and J. Galea, *J. Power Sources* **11** (1984) 7.
- [9] F. Mansfeld and S. Gilman, *J. Electrochem. Soc.* **117** (1970) 1328.
- [10] A. Himy and R. Karcher, Extended Abstract No. 90, Electrochemical Society Fall Meeting, Hollywood, FA (October 1980).
- [11] C. Biegler, R. L. Deutscher, S. Fletcher, S. Hua, and R. Woods, *J. Electrochem. Soc.* **130** (1983) 2303.
- [12] P. N. Ross, 'Feasibility Study of a New Zinc-Air Battery Concept Using Flowing Alkaline Electrolyte', Lawrence Berkeley Laboratory Report, No. LBL-21437 (1986).
- [13] P. N. Ross, 'A New Concept Using Flowing Alkaline Electrolyte', Lawrence Berkeley Laboratory Report, No. LBL-24181 (1987).
- [14] M. Pourbaix, 'Atlas of Electrochemical Equilibria in Aqueous Solutions', National Association of Corrosion Engineers, Houston TX (1974).
- [15] J. O'M. Bockris, Z. Nagy and A. Damjanovic, *J. Electrochem. Soc.* **119** (1972) 285.
- [16] J. Hendriks, A. Van Der Putten, W. Visscher, and E. Barendrecht, *Electrochimica Acta* **29** (1984) 81.
- [17] T. P. Dirkse, *J. Electrochem. Soc.* **126** (1979) 541.
- [18] J. P. G. Farr and N. A. Hampson, *J. Electroanal. Chem.* **13** (1967) 433.
- [19] I. Epelboin, M. Ksouri, and R. Wiart, *J. Electrochem. Soc.* **122** (1975) 1207.
- [20] J. Bressan and R. Wiart, *J. Appl. Electrochem.* **9** (1979) 43.
- [21] A. N. Frumkin, 'Advances in Electrochemistry and Electrochemical Engineering', Vol. 3, (edited by G. W. Tobias and P. Delahay), John Wiley & Sons, New York (1963).